Direct strength prediction of innovative corrugated columns

A. N. Ajamyan, M. Nassirnia, A. Heidarpour & X.L. Zhao
Department of Civil Engineering, Monash University, Melbourne, Australia

L. Gardner
Department of Civil and Environmental Engineering, Imperial College London, London, UK

ABSTRACT: This paper responds to the need for a theoretical model to describe the structural strength capacity of innovative hollow corrugated columns consisting of four cold-formed corrugated mild steel plates. Interest in these columns has been growing over a number of years, due to high ratio of axial load bearing capacity to weight. The paper utilises the Direct Strength Method (DSM) to calculate the axial strength of aforementioned columns while the results are compared with those obtained from experiments and finite element models. Existing formulations are extended to predict local failure of these columns over a vast range of slenderness with a good degree of accuracy. The results show the appropriateness of this method as an alternative for analytical capacity prediction of innovative corrugated columns.

1. INTRODUCTION

Thin-walled structures are a favourable option in the construction of structural elements such as columns as they are lightweight and tend to carry higher structural loads. These favourable attributes of thin-walled columns may have the influence of opening new avenues for mega-structures and larger infrastructure projects. From the other side, optimising the design of steel sections for strength and other requirements can increase safety, decrease cost, minimise resource consumption, and generally provide a better engineering solution. This research focuses on the use of corrugation style to improve the structural performance of mild steel flat plates

In this study, innovative hollow corrugated columns consist of four corrugated mild steel plates, are welded together using butt weld. Each of four corrugated steel plates are produced from 3 mm thick flat mild steel plates, and corrugated through a cold-forming process. This set-up is shown in Figure 1a. In Figure 1b, the geometric layout for comprising plates is depicted.

Corrugated columns have already demonstrated to absorb higher amount of energy, which can be beneficial in structures that are subjected to impact loading, wind and earthquake loads (Nassirnia et al., 2017b). Innovative hollow columns, having a substantial structural capacity, are relatively easy and cheap to be produced, in comparison to the conventional welded box sections.

The structural behaviour of columns formed with corrugated mild-steel plates was first investigated by Nassirnia et al. (Nassirnia et al., 2015). Tensile tests demonstrated significant material enhancements during the cold forming of corrugations, which contributed to axial loading at least two times greater than conventional columns. A finite element model was developed and verified with experimental results. Preliminary cost-benefit analyses indicated that the structural enhancements of corrugated columns make for an economical introduction to civil construction.

In a recent study, design expressions for the hollow columns were developed based upon the effective width method (Nassirnia et al., 2017a). These were explored for a wider range of corrugation designs, and corroborated with an expanded finite element analysis. The results of this finite element model will be used for verification purposes in this study.

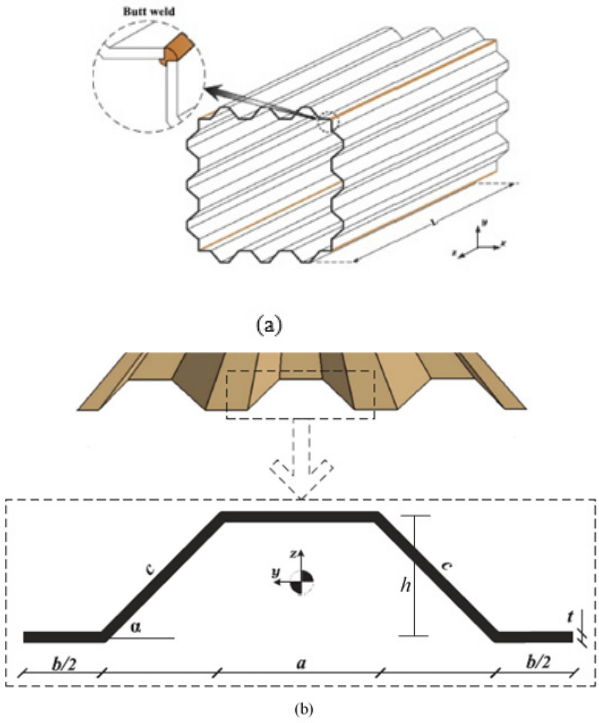

Figure 1: (a) Schematic view of an innovative column, and (b) plat's geometric layout (Nassirnia et al. 2015, 2017a)

In a previous study conducted at Monash University, four cases of corrugated columns were experimentally tested (including a control column, whose plates are not corrugated). Each column was also analysed using Finite Element Model (FEM) on ABAQUS (Simulia, 2012). From both the experimental and finite element models, it was concluded that the geometry of the corrugation has a major impact on the load carrying capacity of the columns (Nassirnia et al., 2015). The two geometric factors that have shown to affect the capacity of the column is the angle (α) and height (h) of the corrugation. Table 1 shows values of differing corrugation angles and heights with their effect on experimental and FEM capacity values.

Table 1: Geometric and load carrying capacity values for innovative columns (Nassirnia et al., 2016)

Column	α (°)	h (mm)	Load carrying capacity (kN) FEM	EXP
Control	-	-	362	371
Case 1	45	15	808	795
Case 2	75	15	848	839
Case 3	75	22	955	953

Note: FEM – Finite Element Model, EXP – Experimental

From Table 1, it can be seen that by increasing the corrugation angle and the corrugation height, the load carrying capacity of the column increases. By corrugating the mild steel sheets, there seems to be a 2.5 times increase in the load carrying capacity of the column, when comparing Case 3 with control.

Asides from the geometric consideration of the column's cross section, there are other attributes that contribute to the load carrying capacity of the column. One of them is due to the Heat Affected Zone (HAZ) of the welding. When welding pieces of metal together, the mechanical properties in and around the weld position change. This creates a residual stress around the weld position, as temperatures of up to 1200°C have been used, which in effect lowers the structural strength and capacity of the column. Another factor is the introduction of cold forming process to the virgin steel plates. These attributes should be taken into account when discussing and interpreting the structural capacity of corrugated columns. Moreover, corrugated sections are made of typical mild-steel plates. As mentioned above, the act of cold forming corrugations enhances material properties at the location of the bend, and so the section cannot be modelled with homogenous strength. Based upon tensile testing results, a yield of 262 MPa is taken for flat strips of the corrugated section and 462 MPa for enhanced regions including corners (Nassirnia et al., 2015). The enhancement is assumed to extend a distance equal to the thickness of the sheet beyond the corner sections, as demonstrated in Figure 2.

The main purpose of this paper is to employ DSM to develop an analytical model to describe the structural strength capacity of innovative hollow columns, which could be useful in the implementation of such columns in the codes of practice.

1.1 *Direct Strength Method (DSM)*

Direct Strength Method (DSM) has been developed for the sole purpose of analysing the structural capacity of thin walled structures and elements and to simplify the current complexity for the analysis of cold formed steel members. DSM provides a more robust and flexible design procedure which integrates current and established numerical models (Schafer, 2008).

DSM was developed for cold-formed steel sections as an alternative to the sometimes cumbersome effective width method. Part of this simplicity comes from DSM's use of gross section properties, rather than effective section properties, which avoids the iteration that characterises effective width method calculations. DSM is applicable to a wider and larger library of cross sections. Most importantly, DSM provides a rational and analytical procedure for sections that have not been studied (American Iron and Steel Institute, 2004a).

Currently, Australian Standards AS4600 section 7.2.1 describes the steps required to calculate the structural capacity of cold formed structures. However, these equations have been developed for open thin-walled members. DSM bypasses this restriction, as it can analyse various cross sections. However DSM does require the elastic buckling behaviour of the member and from that, a series of ultimate strength curves developed to predict the strength of the section (Schafer, 2008).

The characteristics of this study that make DSM an attractive method to investigate the behaviour of corrugated sections are the complexity of these sections under analysis and DSM's more sophisticated approach to different elastic buckling loads. Firstly, the multiple segments of a corrugated section make analysis based upon effective width unwieldy. Secondly, DSM better addresses distortional buckling, ensuring that any solutions are as accurate as possible. Compared to a full spectrum finite element analysis, DSM is computationally less demanding, and has benefits for use in industry as it presents a closed-form solution.

In order to develop formulations which describe the innovative hollow sections, the CUFSM program (Schafer and Ádány, 2006) has been utilised. This program applies the theory of DSM on

inputted cross section. In order to assess the credibility of the program, the experimentally tested columns were modelled on CUFSM.

The method of DSM works on the principle of elastic buckling behaviour. Elastic buckling behaviour can be categorised into three different classes: Local, distortional and global. Local buckling shows a significant distortion of the cross section, however there is no translation at cross-section. Distortional bucking also shows a significant distortion of the cross section, however distortional buckling shows both rotation and translation of the cross section. Global buckling doesn't involve a distortion of the cross section, however there is instead a translation (flexure) and/or rotation (torsion) of the entire cross section. Within this study, these three modes of buckling are utilised by DSM to determine the structural capacity of the innovative columns, and ultimately the formulation of equations to determine the structural capacity of these columns.

DSM has attributes in analysing thin-walled structures, however, it does have a few limitations in both theory and practice. DSM doesn't provide provisions to shear, web crippling and members that contain holes as well as no provisions for noticeable strength increase due to cold-work of forming of sections. DSM also has a limited number of geometries for pre-qualified members. DSM can also deliver an over conservative estimate of strength capacity if given members are very slender (American Iron and Steel Institute, 2006). In terms of using CUFSM, the cross-section and loads cannot vary along the length of the member. CUFSM can only deal with members that are pinned or simply supported (American Iron and Steel Institute, 2006). Even though these limitations can have a small effect on the data that CUFSM will produce, the method of DSM can be regarded as the most suitable method when dealing with thin-walled structures, like those which will be studied in this paper.

2. DSM DEVELOPMENT AND ANALYSIS

2.1 *Evaluation of Innovative column stresses*

Before any analysis of the innovative columns can be made, the average stress of each column is needed. Table 2 shows the geometric properties of all the innovative columns investigated in this study, which will be used to calculate the average stress across each cross-section. A total of 23 column cases were investigated throughout this study, each with a different geometric layout. The angle of corrugation, thickness of the plates, corner radius, and flat region lengths are needed as inputs in order to calculate the yield stress of the column. The following equations are used to evaluate the yield stress for any innovative column configuration:

$$L_E = [(r_c \cdot a) + (2t)] \cdot n \tag{1}$$

$$L_F = 3a + 3b + 6c \tag{2}$$

$$L_U = L_F - L_E \tag{3}$$

$$\sigma_0 = \frac{[(L_E \sigma_E) + (L_U \sigma_F)]}{L_F} \tag{4}$$

where L_E is the enhanced length, r_c is the corner corrugation radius, α is the angle of corrugation, t is the thickness of the plate, n is the number of corners (which is 4 for a single corrugated unit), a, b and c are geometric properties of each column (shown in Table 2), L_U is the unstiffened length of the plate, L_F is the flat region length of the plate, σ_0 is the average yield stress of the cross section, σ_E is the enhanced yield stress and σ_U is the flat region yield stress. It is noted that the enhanced length is defined as the length of the metal plate that has undergone corrugation while the unstiffened length is the length of the metal plate that hasn't undergone corrugation.

Table 2: Geometric properties of the innovative columns investigated

Column Case	α	r_c	a	b	c	h
Case 1	45	7	20	20	21.21	15
Case 2	75	4.75	25.7	25.7	15.53	15
Case 3	75	4.75	18.44	18.44	22.78	22
Case 4	15	7	20.63	20.63	20.63	5.34
Case 5	25	7	20.63	20.63	20.63	8.72
Case 6	10	7	20	10	25	4.34
Case 7	10	7	10	10	10	1.74
Case 8	20	7	20	20	20	6.84
Case 9	20	7	15	15	15	5.13
Case 10	90	7	25	25	25	25
Case 11	90	7	20	20	20	20
Case 12	80	7	40	40	60	59.09
Case 13	80	7	30	30	30	29.54
Case 14	15	7	12	12	13	3.35
Case 15	15	7	20	20	10	2.59
Case 16	10	7	20	20	12	2.08
Case 17	85	7	35	35	40	39.85
Case 18	75	7	20	40	40	38.64
Case 19	60	7	30	30	40	34.64
Case 20	65	7	40	30	40	36.25
Case 21	70	7	40	40	30	28.19
Case 22	85	7	40	40	30	29.89
Case 23	55	7	30	40	40	32.77

Note: α is the corrugation angle (in degrees), r_c is the corner corrugation radius, a, b and c are specific geometric properties and h is the corrugation height (all length dimensions are in mm)

Table 3 shows each column with its corresponding enhanced length, unstiffened length and yield stress. It is assumed that the thickness of the corrugated sheet used for each case is 3mm and the corner radii is 7 mm (excluding Case 2 and 3, where the corner radius is taken as the measured value of 4.75 mm). It is also assumed that the flat region yield will be taken as 262 MPa, while the enhanced yield will be 423 MPa for every case (excluding Case 2 and 3, where the values is taken from experiments as 462 MPa). There is a difference in both corner radii and enhanced yield values when Case 2 and 3 are compared with the rest of the cases studied. (Nassirnia et al., 2015) had measured the corner radii and enhanced yield stresses for Cases 1 to 3 and the results showed that the yield of the column is related to the corner radius. Therefore through coupon tensile experiments, enhanced yield stresses were found for Case 2 and 3 to be the same. The corner radii for Case 2 and 3 were also found to be the same. For the remaining cases that weren't experimentally tested, a constant radius value is used (corner radius for Case 1). The same can be said for the enhanced yield stress. The value of the average yield stress shown in Table 3 was then used to calculate the load that is applied to each innovative column, which was then used to in DSM calculations.

Table 3: Yield stress values for each innovative column studied

Column Case	L_E (mm)	L_U (mm)	σ_0 (MPa)
Control	-	-	262
Case 1	138.0	109.3	352
Case 2	146.6	100.8	381
Case 3	146.6	100.7	381
Case 4	94.0	153.6	323
Case 5	108.7	138.9	333
Case 6	86.7	153.3	320
Case 7	86.7	33.3	378
Case 8	101.3	138.7	330
Case 9	101.3	78.7	353
Case 10	204.0	96.1	371
Case 11	204.0	36.1	399
Case 12	189.3	410.7	313
Case 13	189.3	170.7	347
Case 14	94.0	56.0	363
Case 15	94.0	86.0	346
Case 16	86.7	105.3	335
Case 17	196.6	253.4	332
Case 18	182.0	238.0	332
Case 19	160.0	260.0	323
Case 20	167.3	282.7	322
Case 21	174.6	245.4	329
Case 22	196.6	223.0	337
Case 23	152.6	297.4	317

2.2 *CUFSM*

CUFSM software works by initially inputting the desired cross-section, modelled through nodes linked up by elements with a specific material and thickness, as defined by the user. For this study, the material properties in Table 4 are used for each column case.

Table 4: Material Properties utilised in CUFSM

E_x (MPa)	E_y (MPa)	v_x	v_y	G_{xy} (MPa)
209000	209000	0.3	0.3	80385
Note: E – Modulus of Elasticity, G – Modulus of Rigidity				

The points over which the column will be evaluated on must then be specified. By decreasing the number of points over which CUFSM iterates on, the attained results will be more accurate, however the computation time increases. After inputting the number of points, the column is analysed through the method of DSM. The output of CUFSM is a signature curve of the column cross-section (Schafer and Ádány, 2006). The signature curve contains information which is crucial in determining the load carrying capacity of innovative columns. The horizontal axis of the signature curve is length, while the vertical axis is the load factor. Within the signature curve, there are a number of dips. These dips correspond to particular characteristics of the column under loading. The first dip which usually occurs in the signature curve corresponds to the local buckling of the column and the second dip corresponds to the distortional buckling of the column. The asymptotic behaviour of the signature curve demonstrates the global buckling behaviour of the column (for which the Euler buckling formula can be utilised). Each minima observed on the signature curve has a corresponding load factor value which corresponds to each of the buckling modes. For the global buckling mode, the load factor is calculated through the use of the Euler buckling formula, as shown below (Australian Standard As4100, 1998):

$$P_E = \frac{\pi^2 EI}{(k_e l)^2} \tag{5}$$

where P_E is the buckling load, E is the modulus of Elasticity, taken as 209000 MPa in this work, I is the second moment of area (mm^4), k_e is member effective length factor (taken as 1, as column is pin-pin) and l is the length of the member taken as 1000 mm in this study. Initially, the control and the three cases of innovative columns were tested using CUFSM. This is to ensure that the software package gives approximate values to those obtained through experimental and finite element model investigations, as well as calibrating CUFSM to further investigate other column configurations.

3. RESULTS

Table 5 shows all the cases that were considered in this study, along with their geometric properties, local and distortional factors obtained from CUFSM, design strength capacity (ϕP_n), slenderness values for local, distortional and global buckling as well as the load factors obtained from CUFSM. The method for how to calculate the design strength capacity can be found in the Direct Strength Method Design guide (American Iron and Steel Institute, 2006). From Table 5, an observation is made with respect to the four columns that were experimentally tested. It is observed that the control and the first three innovative cases have slightly different values of design capacity loads (ϕP_n) than those found through experiments and finite element models. This is due to the way that global buckling factor was calculated. Global buckling in a column governed by Euler buckling (equation 5) is used to calculate the global buckling load factor.

The results in and the analysis through CUFSM further solidifies the fact that as we increase the angle of corrugation, the load carrying capacity of the column also increases. For example, those cases that have 90° corrugation angles are seen to have the largest design strength capacity when compared with other cross sections that have low corrugation angles.

Within this report, the torsional buckling failure mode is ignored. As mentioned before, torsional buckling failure doesn't appear for closed innovative sections. Also, the load factor corresponding to distortional buckling is much higher than that of local buckling, which means that local buckling failure is governing the failure mode of closed innovative columns.

4. FORMULATION AND DISCUSSION

Since the main purpose of this study is to formulate a new set of equations which describe innovative columns, both local and distortional buckling factors extracted from CUFSM are utilised to create a set of points.

4.1 *Local and Distortional buckling comparison*

Before any investigation into the desired formulation, further data analysis was conducted. This included the calculation of the flexural/torsional/torsional-flexural buckling load (P_{ne}), P_{test}/P_y (which corresponds to λ_d) and P_{test}/P_{ne} (which corresponds to λ_l). The values of P_{test} are the tested or verified loads for each case. Figure 3 shows a plot of λ_l against P_{test}/P_{ne}. This is very similar to the analysis done for open channels (American Iron and Steel Institute, 2004b), to verify that the design strength equations given in AS4600 are valid. Figure 3 shows the data relationship for local buckling for the innovative columns under investigation.

Table 5: Calculated CUFSM and Direct Stiffness Method values for each innovative column investigated

Column Case	P_{test} (kN)	P_y (kN)	P_{crl}/P_y	P_{crd}/P_y	P_{cre}/P_y	λ_d	λ_l	ϕP_n (kN)
Control	371	778.14	0.424	7.845	80.38	0.36	1.53	417.82
Case 1	795	1043.95	1.568	6.5523	47.94	0.39	0.80	866.32
Case 2	839	1129.63	1.722	5.8309	32.56	0.41	0.76	947.93
Case 3	953	1129.45	2.464	10.022	24.1	0.41	0.63	943.50
Case 4	612	1017.52	0.654	6.485	66.73	0.39	1.23	634.83
Case 5	741	988.24	0.991	6.784	60.81	0.38	1.00	708.57
Case 6	561	921.99	0.629	7.157	62.59	0.37	1.26	567.34
Case 7	417	544.71	1.62	12.79	13.17	0.28	0.77	448.52
Case 8	667	950.31	0.882	7.026	58.99	0.38	1.06	655.59
Case 9	572	881.03	1.043	7.561	33.26	0.36	0.97	639.90
Case 10	1292	1479.86	2.407	4.548	27.21	0.47	0.64	1238.68
Case 11	1084	1148.59	2.942	6.329	15.90	0.40	0.58	950.94
Case 12	2165	2252.1	1.383	3.092	134.33	0.57	0.85	1803.21
Case 13	1435	1497.54	1.812	4.687	54.50	0.46	0.74	1263.17
Case 14	479	653.19	1.342	10.545	21.28	0.31	0.85	512.29
Case 15	484	747.51	0.898	9.069	32.15	0.33	1.05	516.66
Case 16	465	771.08	0.740	8.686	38.06	0.34	1.16	500.22
Case 17	1733	1794.66	1.694	3.956	71.28	0.50	0.77	1516.53
Case 18	1604	1672.02	1.761	4.324	74.36	0.48	0.75	1413.24
Case 19	1559	1629.53	1.331	4.158	113.66	0.49	0.87	1288.56
Case 20	1706	1738.01	1.250	3.920	124.70	0.51	0.89	1347.09
Case 21	1570	1657.86	1.193	4.072	109.26	0.50	0.91	1265.53
Case 22	1625	1700.34	1.411	4.072	79.29	0.50	0.84	1368.21
Case 23	1645	1709.69	1.096	3.874	149.60	0.51	0.95	1270.69

Note: P_y is the calculated load, P_{test} is the test or verified FEM load, P_{crl}/P_y, P_{crd}/P_y, and P_{cre}/P_y ratios are the local, distortional, and global buckling load factors respectively, P_{cre} is calculated using equation 5, λ_d is the distortional buckling slenderness ratio (DSM), λ_l is the local buckling slenderness ratio (DSM) and ϕP_n is the design strength capacity of each column.

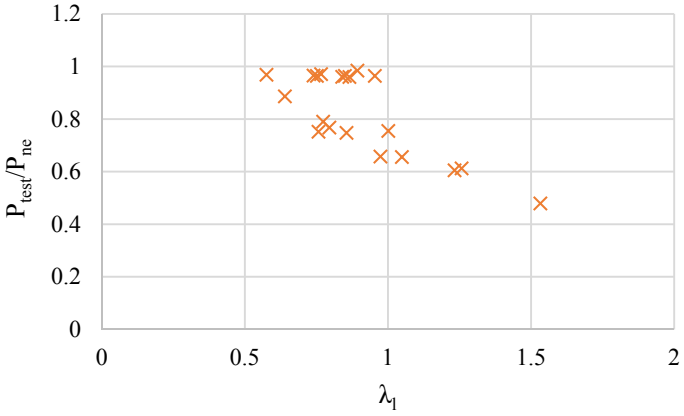

Figure 3: Local Buckling Data for given innovative hollow corrugated members (Nassirnia et al., 2017a)

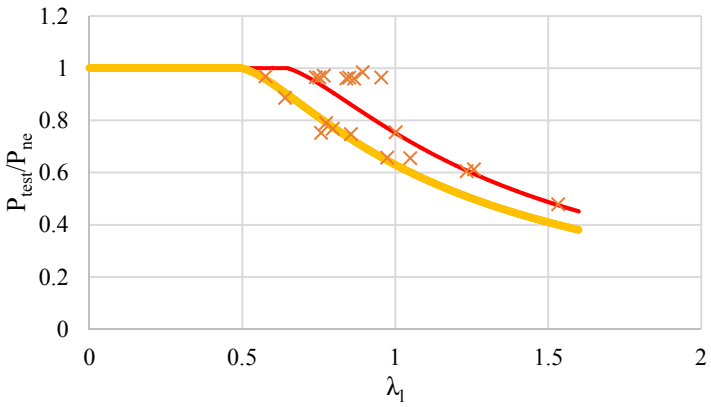

Figure 4: Fitted Mathematical model to mean of local buckling data set (equation 11 - red) and lower bound model of local buckling data set (equation 12 – yellow)

The local buckling data follows a noticeable curve, which is consistent with previous thin-walled members (American Iron and Steel Institute, 2004b).

The DSM calculations showed that for each case, the local buckling mode showed the lowest design capacity for the innovative columns. This is common, as the columns were modelled as being only 1 m long, and therefore distortional buckling effects would not have a large impact on the major buckling mode of the column. Therefore, for this reason, the design capacity equation for these innovative columns will be modelled based on the local buckling data set. A further study may attempt to find the mathematical relationship for the distorional buckling mode of innovative hollow columns, however this would ultimately require more cases to be introduced.

4.2 *Formulation for Innovative Columns*

Following from Figure 3, a mathematical model is to be introduced that will fit the given local buckling mode data set. The final mathematical model will follow the following form:

$$\frac{P_{test}}{P_{ne}} = \left[\varepsilon - \eta\left(\frac{P_{crl}}{P_{ne}}\right)^{\kappa}\right] \cdot \left(\frac{P_{crl}}{P_{ne}}\right)^{\xi} \tag{6}$$

where P_{crl} is the critical elastic column bucking load, P_{ne} is the nominal capacity of a member in compression for flexural, torsional or flexural-torsional buckling (American Iron and Steel Institute, 2004a), P_{test} is the verified compression load value and ε, η , κ and ξ are constants which will be determined through curve fitting process. This equation has the same form as that of the equation given in AS4600 cl 7.2.1.3(2) (Australian Standard As4600, 2005), however to make the model more general, three variables have been introduced. These variables will determine the new fitting model for the given data set. Equation 6 can be further simplified, by using the relationship from DSM, given in equation 7:

$$\lambda_l = \sqrt{\frac{P_{ne}}{P_{crl}}} \tag{7}$$

where λ_l is the slenderness ratio at local buckling. By substituting this relationship into equation 6, the following relationship is:

$$\frac{P_{test}}{P_{ne}} = \left[\varepsilon - \eta\left(\frac{1}{\lambda_l^2}\right)^{\kappa}\right] \cdot \left(\frac{1}{\lambda_l^2}\right)^{\xi} \tag{8}$$

Matlab was used in order to find the corresponding constants. An inbuilt function called Curve Fitting (Matlab, R2013a) was utilised to firstly fit a curve through the data and then using the fitted model, finding the required constants. The model which will be determined through the method of curve fitting will develop a mathematical relationship, which will evaluate the strength capacity of these sections.

From the curve fitting toolbox, MATLAB gives a range of values for each coefficient. From using these ranges, a suitable selection was made to fit the data. The chosen curve must also take into account that at some determined local buckling slenderness point ($\lambda_l \leq \gamma$, where γ is a value that also requires to be determined), the value of P_{test}/P_{ne} will be of value 1. The newly formulated curve will be a piecewise function, satisfying:

$$\frac{P_{test}}{P_{ne}} = \begin{cases} 1, & \lambda_l \leq \gamma \\ \left[\varepsilon - \eta\left(\frac{1}{\lambda_l^2}\right)^{\kappa}\right] \cdot \left(\frac{1}{\lambda_l^2}\right)^{\xi} & \lambda_l > \gamma \end{cases} \tag{9}$$

Where ε, η and κ are constants which will be determined through curve fitting. From the range of

values that the curve fitting tool has provided, as well as the use of trial and error of values between the limits that MATLAB had developed for each of the constants, the following formula is obtained:

$$\frac{P_{test}}{P_{ne}} = \begin{cases} 1, & \lambda_l \le 0.65 \\ \left[1 - 0.248\left(\frac{1}{\lambda_l^2}\right)^{0.7}\right] \cdot \left(\frac{1}{\lambda_l^2}\right)^{0.7} & \lambda_l > 0.65 \end{cases} \quad (10)$$

Equation 10 can be written in the original format:

$$\frac{P_{test}}{P_{ne}} = \begin{cases} 1, & \lambda_l \le 0.65 \\ \left[1 - 0.248\left(\frac{P_{crl}}{P_{ne}}\right)^{0.7}\right] \cdot \left(\frac{P_{crl}}{P_{ne}}\right)^{0.7} & \lambda_l > 0.65 \end{cases} \quad (11)$$

Therefore from equations 10 and 11, it can be seen that $\varepsilon = 1$, $\eta = 0.248$ and $\kappa = \xi = 0.7$.
Figure 4 shows the fitted curve on the local buckling data. As the data is highly variable, the fitted curve does not align with all points. This will cause discrepancies between pretending strength values and those measured from tests.

Equation 11 is derived from fitted models to the mean of all data. For design purposes, another curve is generated which constitutes the lower bound design curve for the innovative columns. Equation 12 models the lower bound design curve of the innovative columns shown in Figure 4.

$$\frac{P_{test}}{P_{ne}} = \begin{cases} 1, & \lambda_l \le 0.495 \\ \left[1 - 0.37\left(\frac{P_{crl}}{P_{ne}}\right)^{0.38}\right] \cdot \left(\frac{P_{crl}}{P_{ne}}\right)^{0.71} & \lambda_l > 0.495 \end{cases} \quad (12)$$

Therefore from equation 12, it can be seen that $\varepsilon = 1$, $\eta = 0.37$ and $\kappa = 0.38$ and $\xi = 0.71$.

CUFSM has been programmed to effectively calculate very simple cross sections, most notably open channels such as C-sections and Z-sections. By modelling closed sections, CUFSM may produce values that are not entirely accurate, and this will propagate through to the mathematical fitting of the data. This propagation will affect the values of P_{test} that will be evaluated, and therefore a difference will be noticed when attempting to validate finite element P_{test} values to those evaluated through the newly founded mathematical model. Also it seems that all of the cases studied were not of sufficient slenderness, as none of the cases showed a P_{test}/P_{ne} ratio of 1. This affects the accuracy of both the limiting value of the local buckling slenderness value as well as the mathematical formulation of the strength capacity of innovative sections.

The introduction of more cases may provide a more in-depth insight into the structural strength capacity of hollow corrugated columns. This will allow a more accurate mathematical model to be derived, as more data points will be made available, closing the large gap between data points and the proposed model. This will ultimately increase the accuracy of how the mathematical model will describe the structural capacity of a particular hollow column.

The introduction of additional cases must also include cases that are significantly slender.

Throughout this study, a common average stress value was used at each corrugated joint (441MPa). However, this doesn't account for the fact of the HAZ (Heat Affected Zone) of the welding as well as the cold-forming process of the corrugation. Even though the average stress value taken may seem to counter act imperfections of the column cross-section, it may be the case that one of the imperfections may have more of an impact on the structural capacity than the other.

To increase the validity of the mathematical model, more cases need to be introduced. In addition to the proposed increase in cases, a more in-depth analysis in correctly modelling the stresses within the section on CUFSM, with respect to the HAZ of the weld and the enhancement of the cold-formed folding of the metal may be a topic for further research.

Distortional failure modes were not critical in the 24 cases analysed, and the columns exhibited a small range of distortional slenderness. As a consequence, the results are not readily extendable to predicting distortional failure. One of the advantages of the DSM formulation is its improved treatment of distortional failure, and so this attempt has not taken full advantage of the methodology selected. DSM still has benefits of computational ease when compared to a more typical effective width analysis and so this concern does not erase the value of this approach.

Going forward, a wider variety of innovative columns could be investigated to provide the basis for a more comprehensive analytical toolkit. This should focus on expanding understanding of both compact columns and distortional failure.

5 CONCLUSIONS

This paper has discussed the need into the study of innovative columns, and the importance of these in structural applications and a new analytical way in determining the structural capacity of such columns.

By utilising DSM, a computing tool, CUFSM, was utilised to study hollow corrugated columns

CUFSM was utilised to find bucking load factors for innovative hollow columns. These load factors were then used through the DSM calculations to evaluate the design strength of each innovative hollow column. The design strength capacity loads were slightly different from those found in both experimental and finite element models, as global elastic buckling was introduced into DSM calculations. From the DSM calculations, it was also determined, that local buckling determined the structural capacity of each column.

The formulation of the structural strength capacity of innovative hollow corrugated columns utilised the slenderness values calculated through DSM for each column case. These slenderness values along with a ratio of load test values to global load buckling was plotted, and a mathematical model was fitted to the data.

An introduction of more cases in a further study with an attention to the HAZ of the welding and enhancements of the cold-forming corrugation in CUFSM, may increase the accuracy of the fitted model.

ACKNOWLEDEGEMENT

This research work was supported by the Australian Research Council through Discovery Projects DP130100181 and DP150100442.

REFERENCES

American Iron and Steel Institute 2004a. Appendix 1: Design of Cold-Formed Steel Structural Members using the Direct Strength Method. *Specification for the Design of Cold-Formed Steel Structural Members*.

American Iron and Steel Institute 2004b. Commentary on Appendix 1: Design of Cold-Formed Steel Structural Members with the Direct Strength Method. *Specification for the Design of Cold-Formed Steel Structural Members.*

American Iron and Steel Institute 2006. Direct Strength Method (DSM) Design Guide *Committee on Specifications for the Design of Cold-Formed Steel Structural Members*.

Australian Standard As4100 1998. AS4100 - Steel structures. *Standards Australia, NSW, Australia.*

Australian Standard AS4600 2005. AS4600 - Cold-formed Steel Structures. *Standards Australia, NSW, Australia*. Australian Steel Institute.

Matlab R2013a. CurveFitting Toolbox. Natick, Massachusetts, United States: The MathWorks, Inc.

Nassirnia, M., Heidarpour, A. & Zhao, X.-L. 2017a. A benchmark analytical approach for evaluating ultimate compressive strength of hollow corrugated stub columns. *Thin-Walled Structures,* 117: 127-139.

Nassirnia, M., Heidarpour, A., Zhao, X.-L. & Minkkinen, J. 2015. Innovative hollow corrugated columns: a fundamental study. *Engineering Structures,* 94: 43-53.

Nassirnia, M., Heidarpour, A., Zhao, X.-L. & Minkkinen, J. 2016. Innovative hollow columns comprising corrugated plates and ultra high-strength steel tubes. *Thin-Walled Structures,* 101:14-25.

Nassirnia, M., Heidarpour, A., Zhao, X.-L., Wang, R., Li, W. & Han, L.-H. 2017b. Experimental Behavior of Innovative Hollow Corrugated Columns under Lateral Impact Loading. *Procedia Engineering,* 173: 383-390.

Schafer, B. W. 2008. The direct strength method of cold-formed steel member design. *Journal of constructional steel research,* 64: 766-778.

Schafer, B. W. & Ádány, S. Buckling analysis of cold-formed steel members using CUFSM: conventional and constrained finite strip methods. Eighteenth international specialty conference on cold-formed steel structures, 2006. 39-54.

Simulia 2012. Abaqus Software Package. Providence (RI).